

Optimization of high energy intensity systems, case study: Electric arc furnace

AMIRHOSSEIN FATHI¹, HOSSEIN YOUSEFI^{2,*}, NIMA MAHDIAN DEHKORDI³, AND KIANOOSH CHOUBINEH²

¹School of Mechanical Engineering, Shiraz University, Shiraz, Iran

²Department of Renewable Energies and Environment, Faculty of New Sciences and Technologies, University of Tehran, Tehran, Iran

³Department of Control Engineering, Shahid Rajaei Teacher Training University, Tehran, Iran

* Corresponding author email: hosseinyousefi@ut.ac.ir

Manuscript received 19 April, 2021; revised 06 October, 2021; accepted 17 November, 2021. Paper no. JEMT-2104-1295.

This study initiates a framework to indicate the optimal inputs into complex, high-energy intensity systems. It has a lower computational load, higher reliability, and better accuracy. The lower load comes from the developed linearization algorithm of a system. There is the ability to match every output to input to reach reliability, and a sophisticated algorithm guarantees accuracy. An Electric Arc Furnace model is chosen to validate the framework because of its nonlinear functions, complexity, and significant energy intensity. The procedure is applied to an EAF model. Liquid mass, liquid temperature, and liquid grade must reach the desired ranges. This step is to be accomplished at the lowest cost in a determined time. The technique linearizes the nonlinear model around an operating point in the first step and reduces the system's order. A suitable pairing is based on minimum interaction and passing some necessary decentralized integral controllable requirements in the second step. The third step is based on discretizing the operating point's linearized system. The algorithm is repeated around new operating points. A comparison between the nonlinear system and reduced linear ones with the same feeds is made in any iteration. If the results are compatible, the next optimum feeds are estimated. Otherwise, the sample time decreases, and the loop is reiterated for the previous point. The method is carried out on a well-known EAF model with 14 state variables and seven input variables. The outcomes also are adaptable with the nonlinear model. They also suggest compound simulation models can be transformed into simpler ones with little effect on implementing control structure results. © 2022 Journal of Energy Management and Technology

keywords: Energy-material flow optimization, high energy intensity, reliability, low computational load smart grid.

<http://dx.doi.org/10.22109/jemt.2022.282062.1295>

NOMENCLATURE

i, j, k	Index of cluster.
m	Feature index for elements of x_i .
$N_{Cluster}$	Total number of clusters.
$N_{dataset}$	Number of members of the dataset.
N_f	Number of features.
c	Cluster's centroid.
c_{c1}, c_{c2}	Centroids of first and second clusters, respectively.
n_i, n_j, n_k	Number of members of the clusters i, j and k , respectively.
r_a	A positive constant which defines the neighborhood of a data point.
r_b	A positive constant to separate the cluster centers.
a, b, λ	Coefficients.

P_i	Probability of the occurrence of the cluster i .
$Mean_{dataset}$	The mean of the dataset.
D_{base}	Dispersion of base dataset.
S_{factor}	Similarity factor.
D_{x_i}	Density of each data point.
D_{c1}	Density of the first cluster's centroid.
x_i	Each observation in dataset.
$x_i(m)$	The m^{th} feature of the observation x_i .
d_{ik}, d_{jk}, d_{ij}	The pairwise distances between the clusters i and k, j and k , and i and j , respectively.

1. INTRODUCTION

Steel is being produced in more than 65 countries [1], and this alloy contributes to 2.5 percent of world trade. Four reasons

can underline the importance of optimizing the steel industry's consumption and energy, as follows.

1. The iron and steel-making factories are ranked second to the energy-intensive industries [2]. In 2007, a fifth of the industry sector's total energy use was in the steel industry [3].
2. The energy factor's role in the final steel cost is estimated to be nearly 30 % in an integrated system [4]. Various steel manufacturing methods and variations in different countries' production factors cause this role to be 20-40 % of the overall cost [5].
3. Increasing demand: the steel demand is predicted to rise by 2.5 % annually until 2030 [1].
4. The discrepancy between energy intensity and theoretical ideal energy consumption [6]: despite a 60 % reduction in this industry's energy intensity during the last six decades [7], there is a noticeable discrepancy between the actual routine practice and the minimum practical practice [6].

The majority of steel is produced through two routes: blast - basic oxygen furnace and oxygen hearth furnace [7, 8]. The other methods' share, such as oxygen hearth or plasma arc furnace, is insignificant.

Global statistics show that steel making's percentage using an Electric Arc Furnace (EAF) has climbed. The percentage increased from 16.9 %, equivalent to 100.439 million tones, in 1975 [9] to 28.2 %, equivalent to 465.018 million tones, in 2013 [8, 10]. The main reasons behind this global growth are a decrease in annual investment cost for oxygen furnace [11], the end of open furnace production [7, 8], and electric arc furnace improvements [12]. Moreover, compared with the induction furnace, the EAF is used more because of its low sensitivity to iron sources' quality, like scrap, hot charge, Direct Reduced Iron (DRI), and cast iron. Choosing the production's technique, however, relies on available energy resources and materials, demand, and the construction year of a factory [12].

Nemours studies focused on minimizing the utilization of material-energy intensity in EAFs. The strategies proposed by those studies can be classified into four categories: high-efficiency equipment application, heat recovery, correcting production management, and controlling the flow of material-energy. The study concentrates on the last category.

An EAF is a reactor with complex phenomena, high interaction, and batch processes. It is used to convert direct reduced iron (DRI) and scrap into a wide range of steel grades. One cycle of EAF includes six steps: furnace charging, melting, refining, de-slagging, tapping, and furnace turn around [13].

Before tapping, the liquid steel needs to reach a specific temperature, mass, and grade. Steelmaker's profit is affected by energy consumption and tap to tap time. Thus optimum feeds have to cause minimum operation cost associated with satisfying the constraints (mass, temperature, and grade). Many methods have been developed and used to attain the optimum feeds for EAF that can be divided into trial and error, optimal control, and model predictive control. The model-based control, the considered solution method for the optimization problem, and available hardware play a major role in selecting one of the abovementioned methods.

A. Trial and Error

An additional strategy for discovering the optimal inputs is trial and error, which is spot finding. It examines points with a higher probability of the objective function. Guo et al. [14], for example, evaluated the slag height's influences on minimizing

radiation losses.

B. Optimal Control

In this section, the optimization problem is defined to obtain the optimal route with one run. This approach's application is for those problems with low computational load.

MacRosty and Swartz [15] defined the optimal material-energy flow to EAF using mathematical optimization. The furnace operating index was analyzed with profit function, including operational costs and molten grade at the discharge period. The identified model was bounded to the differential-algebraic model of EAF, operation's restrictions, and endpoints' limitations. Several practices were suggested to raise precision and decrease solving time: changing a variable scale for a better numerical condition, logarithmic conversion to prevent small negative quantities that must be positive, and approximating discrete parts with linear ones for diminishing computational load. gPROMS/gOP commercial software was utilized, and the EAF model of this study was a derivation of their previous work [16].

C. Model Predictive Control

The optimal route is determined in pieces by the predictive control approach, investigating systems with a higher computational load.

Bekker et al. [17] achieved the optimal furnace consumption in a particular condition based on an operator's experiences and environmental restrictions. The condition was relative pressure of -5 Pascal, output gas temperature of 500oC, and one percent mass concentration of CO in the exhaust gas. Predictive control was employed to reach target points. Although there was no explanation of why the points were optimal, they were usually considered the optimum.

Oosthuizen et al. [18], with Model Predictive Control (MPC), found the best input path for operating an EAF. The optimization problem comprised the quadratic objective function restricted to a linear EAF model containing input costs and control variables deviation from the optimum, route constraints, and final points. Relative pressure, exhaust gas temperature, slag height, CO percentage in the exhaust gas, dissolved carbon percentage in melted, melted temperature, and mass were control variables. Controlling the furnace variables were the fan's power, canal width and graphite, oxygen, and DRI injection rates.

Saboochi et al. [19] brought up a six-step framework to find the optimal inputs. These steps are: 1) Splitting the discrete process into several continuous ones, 2) Dividing the system of multi input- multi output into imaginary connected subsystems in every operational stage, 3) Defining a multi-objective function consisting of minimum losses and operational costs and maximum useful power, 4) Classifying the losses into two groups, controllable and uncontrollable, and eliminating the uncontrollable part from the objective function, 5) Changing point constraints to path ones owing to separating operational steps and 6) Breaking down the optimization problem into several problems. Useful energy cost and heating time declined by nearly 11.3 % and eight percent, respectively. This strategy adjusted the slag height and arc length during the heating to increase the chemical energy's share against the electrical energy's fraction.

This study focuses on carrying on Coetzee et al.[20] by

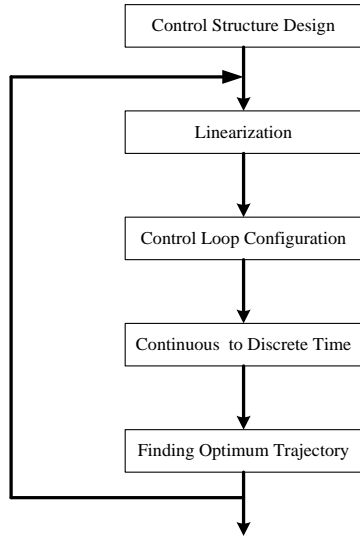


Fig. 1. Control framework.

introducing a method to investigate the optimal inputs into systems through linearizing higher interaction nonlinear models. Operating points can change every moment despite similar studies assessing linearized models around an operating point. In the following section, a structure is first offered to obtain optimum feeds for the nonlinear batch. This algorithm is then implemented on an EAF model to find optimal economic feeds in the refining state. In these circumstances, an EAF is not charged by DRI and flux [20].

2. APPROACH

Fig. 1. shows the suggested control strategy for nonlinear batch processes. The strategy is iterative. In the first step, which is control structure configuration, appropriate inputs and outputs must be determined, and the input and output number should be equal. The system is linearized in the second step. The third is about looking for a proper pairing. In the fourth one, the continuous system is converted to a discrete system. Finally, the optimum feeds are calculated based on the discrete system. The loop will be iterated from the second step up to achieving goals.

A. Control Structure Design

The suggested control strategy is suitable for a linear system. For a system with manipulated variables (M) and controlled variables (N), three cases are presented:

1. $N = M$: the system is decentralized.
2. $N < M$: if some manipulated variables depend on others, the dependent variables are substituted with independent variables. After this, if the residual manipulated variables are more than controlled ones, N manipulated variables must be chosen from residual manipulated variables.
3. $N > M$: it is suggested to remove the N-M controlled variables with lower priorities. Relative Gain Array (RGA) is one of the fitting tools that can be used.

B. Linearization

A nonlinear system, presented by (1), can be linearized around x_0 and u_0 with the help of (2).

$$\dot{x} = F(x, u) \tag{1}$$

$$\dot{x} = \begin{bmatrix} \frac{\partial f_1}{\partial x_1} & \dots & \frac{\partial f_1}{\partial x_n} \\ \dots & \dots & \dots \\ \frac{\partial f_n}{\partial x_1} & \dots & \frac{\partial f_n}{\partial x_n} \end{bmatrix} \bigg|_{x_0, u_0} \Delta x$$

$$\begin{bmatrix} \frac{\partial f_1}{\partial u_1} & \dots & \frac{\partial f_1}{\partial u_n} \\ \dots & \dots & \dots \\ \frac{\partial f_n}{\partial u_1} & \dots & \frac{\partial f_n}{\partial u_n} \end{bmatrix} \bigg|_{x_0, u_0} \Delta u + \dot{x}_0 = A\Delta x + B\Delta u + \dot{x}_0 \tag{2}$$

(2) is derived from (3).

$$\dot{x} = A\Delta x + B\Delta u + \dot{x}_0 \tag{3}$$

C. Control Loop Configuration

An appropriate pairing will be introduced by using some rules. A pairing is proper with minimum interaction and is resistive against changing controller coefficient and fault in sensors or actuators.

This section is divided into two subsections. The first part arranges the pairings from the lowest interaction to the highest one, and the other intends to find decentralized integral controllable pairings if they exist. Some indexes, such as Column Dominance Ratio, Perron Frobenius Eigenvalue, RGA, Effective Relative Gain array (ERGA), are utilized to measure interactions. Before applying these methods, the correct pre compensator and post compensator are advised to be carried out.

C.1. Interaction

Scaling methods can be applied to reduce interaction. It is hard to find a fixed operating point in the batch process; changing the working point causes not to be implemented prevalent pre-compensator and post compensator based on Perron Frobenius and Edmund. Unit scaling is strongly recommended so that all elements become near to each other.

Interaction evaluation of each pairing can be executed with a summation of Column Dominance Ratio (CDR) of all loops within a distance of ten times of bandwidth. CDR is calculated by (4).

$$CDR_i(s) = \frac{\sum_{i=1, i \neq j}^m |q_{ij}(s)|}{|q_{ij}(s)|} \tag{4}$$

where, $q_{ij}(s)$ is i th row and j th column element of the transfer function and $CDR_i(s)$ is the column dominance ratio of i th loop.

C.2. Eliminating Non-DIC Pairing

Screening nondesirable pairing takes place with necessary DIC rules. DIC is a property of plant and chosen pairing [21]. It should be considered there is a chance to find or miss a DIC pairing since the model is not fitted to the study, Each model simulates some processes with specific accuracy based on its aim. Changing the method can alternate the suggested pairing. Hence, after calculating the pairing, the experts' and operators' comments are received.

If there is a controller $\frac{1}{s}C(s)$, a closed-loop plant is stable for all $E\frac{1}{s}C(s)$, where $E\frac{1}{s}C(s)$ and $E \in \varepsilon, = \{E = \text{diag}(\varepsilon_i) | \varepsilon_i \in [0, 1], i = 1 \text{ to } m\}$ [22]. Determining DIC pairing is difficult for large plants [23]. Non-DIC pairings are proposed to be screened for these plants. Four popular rules of screening are described as below:

- **First Rule:** Eliminating pairing with a negative state. RGA is one of the level measurements of interaction [24] and is calculated by (5).

$$\Lambda = G(s) \otimes (G^{-1}(s))^T \quad (5)$$

where, \otimes is the Schur product, and G is the transfer function. If computing RGA at steady state is the goal, s must be zero. Pairing with a negative element of λ_{ii} has one of the following properties:

- 1. The closed-loop system is unstable, but without i th loop, the plant can be stabilized [22].
 - 2. The closed-loop system is stable, but if a failure happens corresponding to the i th loop, the plant will become unstable [22].
- **Second Rule:** Eliminating pairing with negative Niederlinski Index (NI). (6) quantifies NI.

$$NI = \frac{|G(0)|}{\prod_{i=1}^n g_{ii}} \quad (6)$$

Pairing with negative NI is unstable. The first and second rules are an essential condition for integrity [22].

- **Third Rule:** Eliminating pairing with negative Morari Index of integral controllability. Calculating the index requires that all diagonal elements of the steady-state gain matrix are positive, or the signs are adjusted to positive. In the second step, the eigenvalue of the changed steady-state gain matrix has to be computed. Pairings with a negative real part of the eigenvalue should be erased because they create an unstable closed system [21]. This index is indicated by (7).

$$MIC = \text{Re} \{ \lambda(G^+(0)) \} \quad (7)$$

where, $G^+(0)$ is a steady-state gain matrix with a positive diagonal.

- **Fourth Rule:** Eliminating pairing with negative $\text{Re} \{ \lambda(G^+(0) * \text{diag}(G^+(0))) \}$. The third and fourth rules are extracted from the DIC theorem. Based on (8), If the system is DIC, the index $(\Omega(G(0)))$ must be non-negative for all values of K .

$$(\Omega(G(0))) = \min_k \min_i \text{Re} \{ \lambda(G^+(0)K) \} \quad (8)$$

K is the matrix of diagonal elements of $G^+(0)$.

D. Discretization

The optimum trajectory is found around a discrete system. A continuous system is converted to a discrete one as written by (9).

$$x(k+1) = A_d x(k) + B_d u(k) + \dot{x}_0 T_s \quad (9)$$

Where, T_s is sample time.

E. Finding the Optimum Trajectory

Optimum feeds are obtained by solving the below mathematics programming model, as stated by (10).

$$\text{Min } Z = \sum_{i=1}^m \sum_{K=1}^N P_i u_i(K)$$

st.

$$x(k+1) = A_d x(k) + B_d u(k) + \dot{x}_0 T_s \quad K = 1 \text{ to } N$$

$$x(N) = x_{\text{desire}} \quad (10)$$

$$\Delta u_{i,\min} \leq u_i(K+1) - u_i(K) \leq \Delta u_{i,\max}$$

$$u_{i,\min} \leq u_i(K) \leq u_{i,\max}$$

where, $u_i(K)$ is i th input at K th point, $u(K)$ is input vector at K th point, $u_{i,\max}$ and $u_{i,\min}$ are the maximum and minimum acceptable value of i th input, $\Delta u_{i,\max}$ and $\Delta u_{i,\min}$ are the maximum and minimum acceptable change of i th input, x_{desire} is the vector of the state variable's desire value at the simulation's endpoint, N is the rang number, m is the number of the manipulated variable. The first constraint in (10) can be modified with (11). In these circumstances, the computation cost diminishes.

$$X_K = M x_K + C U_K + P \dot{x}_0 T_s \quad (11)$$

where, T_s is sample time. M , C and P matrices are calculated by (12) to (14), respectively. X_K and U_K vectors are computed using (15) to (16), correspondingly.

$$M = \begin{bmatrix} A_d \\ A_d^2 \\ \vdots \\ A_d^N \end{bmatrix} \quad (12)$$

$$C = \begin{bmatrix} B_d & 0 & 0 & 0 \\ AB_d & B_d & 0 & 0 \\ \vdots & \vdots & \vdots & \vdots \\ A_d^{N-1} B_d & A_d^{N-1} B_d & \cdots & B_d \end{bmatrix} \quad (13)$$

$$P = \begin{bmatrix} I \\ I + A_d \\ I + A_d + A_d^2 \\ \vdots \\ \sum_{i=1}^N A_d^{i-1} \end{bmatrix} \quad (14)$$

$$X_K = \begin{bmatrix} x_{K+1|K} \\ x_{K+2|K} \\ \vdots \\ x_{K+N|K} \end{bmatrix} \quad (15)$$

$$U_K = \begin{bmatrix} U_{K|K} \\ U_{K+1|K} \\ \vdots \\ U_{K+N-1|K} \end{bmatrix} \quad (16)$$

Where, $x_{K+1|K}$ shows a vector of state variables at the moment of $K+1$ based on information of K 's moment.

3. SIMULATION

Bekker et al.'s model [25] is chosen as a case study. The reason for selecting an electric arc furnace is to show the model's strength in simplifying the process simulation model used in the control system with a low effect on results. There is also no need to be a pairing DIC for each discrete process. This model explains the phenomena in EAF with 14 states. Manipulated variables of the model are oxygen injection rate d_1 , DRI injection rate d_2 , Flux injection rate d_3 , arc power d_4 , the graphite injection rate d_5 , fan power u_1 and slip gas width u_2 . It is crucial to achieve certain liquid mass, liquid temperature, and carbon mass in the refining stage. The manipulated variables in this state are oxygen injection rate, arc power, and graphite injection rate. Table 1 gives the initial condition. It is scheduled that in 6.2 seconds, liquid steel mass and temperature will reach at least 136054.4 kg and 701.36027 K, respectively, and dissolved carbon in liquid metal will be lower than 999.7 kg.

The control loop is iterated every 1.6 seconds in the first part. In any iteration, appropriate pairing is investigated. There are six states of pairings, and they are expressed in Table 2. In the second part, the loop is iterated every four and 16 seconds. At the end of the simulation, the results are compared with the steel quality viewpoint, linearization error, and operating costs, such as energy and raw materials costs.

The first part analyzes a suitable pairing four times. Based on the RGA method, just one pairing shown by (17) can be suggested. In this state, liquid mass, carbon mass, and liquid temperature are paired with graphite injection rate, oxygen rate, and electrical power, respectively. The pairing illustrates a high interaction, and it is not reasonable to use

a decentralized controller.

$$\Lambda = \begin{bmatrix} -8.3E + 15 & -E + 13 & 8.32E + 15 \\ 8.31E + 15 & 1.02E + 13 & -8.3E + 15 \\ 0.1137 & 0.987819 & 0.125879 \end{bmatrix} \quad (17)$$

The results of applying screening tools are briefly stated in Table 3. Each box of the Table contains the pairing's necessary condition.

The proposed strategy is generally described in this study. There is no need to find pairing DIC to reach the input's optimal path. This section was added to the paper because discrete processes do not have constant operating points, and therefore, getting a pairing may not be possible.

Table 4 concisely lays out the two models' comparison.

In the following, the nonlinear system's simulation results and reduced linear system are compared with each other, Fig. 2. Two model inputs are the same.

As it is observed regarding high interaction, a piecewise linear system acts similarly to a nonlinear system.

The second simulation part evaluates the number of loops on:

1. an error of linearizing and reducing the state variables,
2. steel specification,
3. Operating cost.

- **First Comparison: Linearizing and reducing the system order.**

Increasing the number of loops enhances the results since repeating the loop can consider other omitted state variables' effects. Two error indices measure the difference between reduced linearized systems. One of them, (18), shows the error at the end of the simulation, and the other, (19), indicates error accumulation.

$$ME(t) = \left| \frac{Y_{Nonlinear_i}(t) - Y_{Linear_i}(t)}{Y_{Nonlinear_i}(t) - Y_{Initial_i}} \right| * 100 \quad (18)$$

$$AE = \left| \frac{\int_0^T (Y_{Nonlinear_i}(t) - Y_{Linear_i}(t)) dt}{\int_0^T (Y_{Nonlinear_i}(t) - Y_{Initial_i}(t)) dt} \right| * 100 \quad (19)$$

where, $Y_{Nonlinear_i}(t)$ is i th nonlinear system output at t , $Y_{Linear_i}(t)$ is i th reduced linear system output at t , and $Y_{Initial_i}$ is the initial point of i th output.

Table 5 gives errors of linearizing and reducing the system. Decreasing the linear system is the root cause of reducing errors by increasing the loops' number.

The iteration number rise can be interpreted as reducing error due to the linear system's adjustment.

- **Second Comparison: Steel quality**
Table 6 states the liquid steel specification at the end of the simulation. The results are based on the nonlinear system. As seen, the constraints are satisfied in the three cases.

Table 1. Initial conditions

	Description	Amount
x_1	Scrap mass	2000 kg
x_2	Liquid steel (LS) mass	136000 kg
x_3	Dissolved carbon in LS	1000 kg
x_4	Dissolved silicon in LS	850 kg
x_5	Solid slag mass	500 kg
x_6	Liquid slag (LG) mass	9000 kg
x_7	Dissolved iron oxide in LG	650 kg
x_8	Dissolved silicon in IS	600 kh
x_9	Carbon monoxide	11.7 kg
x_{10}	Carbon dioxide	9.1 kg
x_{11}	Nitrogen mass in the freeboard	17.4 kg
x_{12}	liquid temperature	1700 K
x_{13}	Solid temperature	1460 K
x_{14}	Relative pressure	-0.01
	u_1	16.25 kg/s
	u_2	0.2 m
	d_1	2 kg/s
	d_2	0 kg/s
	d_3	0 kg/s
	d_4	80000 KW
	d_5	1

Table 2. The possible pairing of reduced EAF model

	Liquid iron mass	Carbon mass	Liquid temperature
1	Oxygen Rate	Electrical Power	Graphite Rate
2	Oxygen Rate	Graphite Rate	Electrical Power
3	Electrical Power	Oxygen Rate	Graphite Rate
4	Graphite Rate	Oxygen Rate	Electrical Power
5	Electrical Power	Graphite Rate	Oxygen Rate
6	Graphite Rate	Electrical Power	Oxygen Rate

Table 3. Results of applying DIC screening rules

	First Rule	Second Rule	Third Rule	Fourth Rule	Conclusion
First Working Point	3	3, 4	1, 4, 5, 6	6	Non
Second Working Point	4, 6	3, 4, 6	3, 4, 6	3, 4, 6	6
Third Working Point	4	Non	2, 3, 4, 6	5	Non
Forth Working Point	2, 5	1, 2, 5	1, 2, 5, 6	1, 2, 5, 6	5

Table 4. Results of endpoint

	Nonlinear model	Reduced linear model
Liquid steel mass	136054.33291 kg	136054.4000 kg
Liquid steel temperature	1703.4075 K	1703.41713 K
Dissolved carbon mass	998.27747 kg	998.275581kg
Consumed oxygen mass		6.28 kg
Consumed graphite mass		3.462681771 kg
Electric energy consumption		251200 KWh

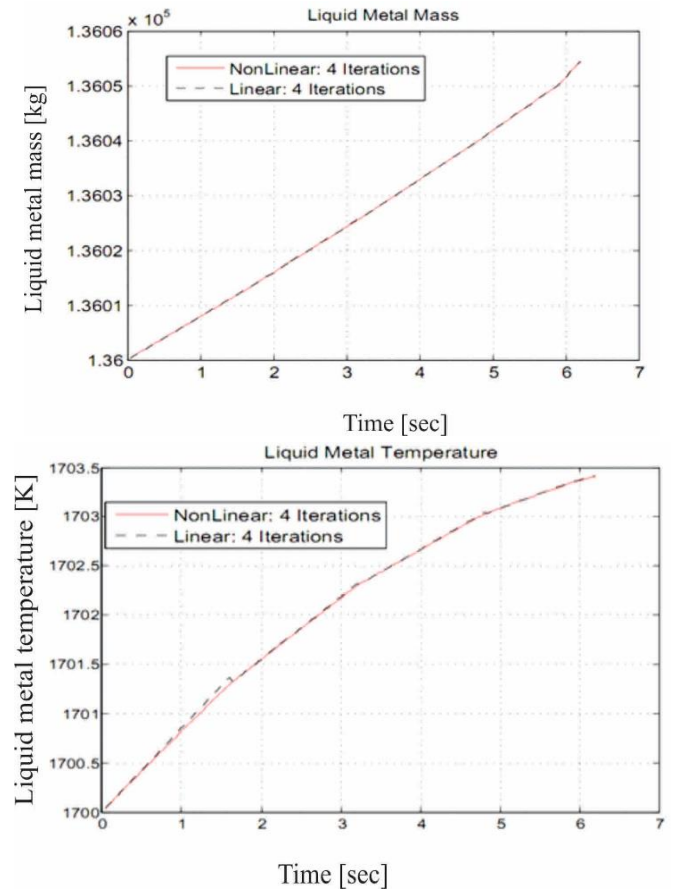


Fig. 2. Liquid steel mass and temperature

- Third comparison: operating cost

Table 7 states the iteration number effect on the operating costs.

Fig. 3 envisage the iteration number with liquid metal mass and liquid temperature.

4. CONCLUSION

This study introduces a framework for identifying the optimal input of complex systems, requiring higher reliability. The input is calculated through conversion to a linear system in a repetitive structure. The linear system is adjusted in each step, and connecting one output to one input examines reliability. Although it is applicable to use this method on simple systems to reduce their energy consumption, its main advantage is for complex ones. EAC is the best instance of an intricate system

Table 5. Expresses the errors of reducing and linearizing the nonlinear model

	One Iteration	Two Iterations	Four Iterations
ME	3.031377556	0.532979131	0.123482468
	1.582313283	0.255751756	0.109596074
	7.462519527	0.35950449	0.2814347
AE	0.081062108	0.018577136	0.002632356
	0.046337438	0.011142076	0.002628229
	0.301097952	0.084113005	0.014397535

Table 6. The liquid steel specification at the end of the simulation

	One Iteration	Two Iterations	Four Iterations	Expectation
Liquid Mass	136052.79945 kg	136054.11160 kg	136054.33291 kg	m >136054.4 kg
Liquid Temperature	1704.839166 K	1704.48487 K	1703.4075 K	T >1701.36027 K
Carbon Mass	998.275937 kg	998.27628 kg	998.27747 kg	m <999.7 kg

with considerable energy intensity and high energy use owing to its production volume.

The case study is an EAF model with 14 states and seven input variables, in which three states are checked for reliability in high interaction cases. The results imply that increasing the iteration number improves errors and cost function because of omitting 11 states. The linearization errors are in acceptable ranges. The interaction measure demonstrates a high interaction between inputs and outputs, and EAF cannot easily be controlled with a decentralized controller.

REFERENCES

- Association WS. World steel in figures 2012. World Steel Assoc 2012.
- Gruenspecht H. International energy outlook 2011. Cent Strateg Int Stud 2010.
- Taylor P. Energy Technology Perspectives 2010. Scenar Strateg To 2010;2050.
- Bisio G, Rubatto G, Martini R. Heat transfer, energy saving and pollution control in UHP electric-arc furnaces. Energy 2000;25:1047–66.
- Association WS. Energy use in the steel industry. World Steel Association; 2014.
- Fruehan RJ, Fortini O, Paxton HW, Brindle R. Theoretical minimum energies to produce steel for selected conditions. Carnegie Mellon University, Pittsburgh, PA (US); Energetics, Inc., Columbia . . . ; 2000.
- Association WS. Fact sheet: energy use in the steel industry. Worldsteel Comm Econ Stud Brussels, Brussels 2016.
- Association WS. World steel in figures 2014. World Steel Assoc 2014.
- A Handbook of World Steel Statistics. 1978.
- Association WS. Annual steel production 1980-2013 2014.

Table 7. Iteration number of affection for operating costs and consumption of feeds

	One Iteration	Two Iterations	Four Iterations
Oxygen Consumption	9.856 kg	8.984 kg	6.28 kg
Electrical Energy Consumption	394240KWh	359360 KWh	251200 KWh
Graphite Consumption	6.093537096 kg	5.677773268 kg	3.462681771 kg
Total Cost	88.98570394 \$	81.60620418 \$	55.01961597 \$

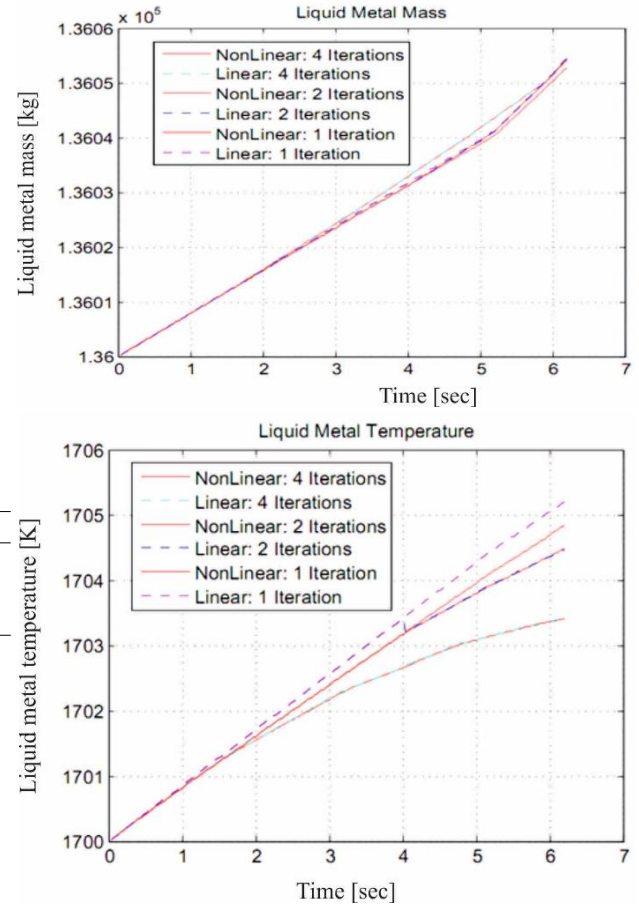


Fig. 3. Liquid steel mass and temperature based on the iteration number

- Wakelin DH, Fruehan RJ. The making, shaping and treating of steel-Iron Making. David H Wakelin, Richard J Fruehan/Latest Technol 1999;2:497–533.
- Toulouevski YN, Zinurov IY. Innovation in electric arc furnaces. Nov lorque Springer 2010:1–23.
- J.A.T. Jones. Electric Arc Furnace Steelmaking 2005.
- Diancai G, Irons A. Modeling of radiation intensity in an EAF. third Int. Conf. CFD Miner. Process Ind. CSIRO, Melbourne, Aust., 2003.
- MacRosty RDM, Swartz CLE. Dynamic optimization of electric arc furnace operation. AIChE J 2007;53:640–53.
- MacRosty RDM, Swartz CLE. Dynamic modeling of an industrial electric arc furnace. Ind Eng Chem Res 2005;44:8067–83.
- Bekker JG, Craig IK, Pistorius PC. Model predictive control of an electric arc furnace off-gas process. Control Eng Pract 2000;8:445–55.
- Oosthuizen DJ, Craig IK, Pistorius PC. Economic evaluation and design of an electric arc furnace controller based on economic objectives. Control Eng Pract 2004;12:253–65.
- Saboochi Y, Fathi A, Škrjanc I, Logar V. Optimization of the electric arc furnace process. IEEE Trans Ind Electron 2018;66:8030–9.
- Coetzee LC, Craig IK, Rathaba LP. MPC control of the refining stage of an electric arc furnace. IFAC Proc Vol 2005;38:151–6.
- Skogestad S, Morari M. Variable selection for decentralized control 1992.
- Khaki-Sedigh A, Moaveni B. Control configuration selection for multi-variable plants. vol. 391. Springer; 2009.
- Haggblom KE. Integral controllability and integrity for uncertain systems. 2008 Am. Control Conf., IEEE; 2008, p. 5192–7.
- Skogestad S, Postlethwaite I. Multivariable feedback control: analysis and design. vol. 2. Citeseer; 2007.

25. Bekker JG, Craig IK, Pistorius PC. Modeling and simulation of an electric arc furnace process. *ISIJ Int* 1999;39:23–32.